

# UC Irvine

## UC Irvine Previously Published Works

### Title

Transmembrane helices containing a charged arginine are thermodynamically stable

### Permalink

<https://escholarship.org/uc/item/8pz877vr>

### Journal

European Biophysics Journal, 46(7)

### ISSN

0175-7571

### Authors

Ulmschneider, Martin B  
Ulmschneider, Jakob P  
Freites, J Alfredo  
et al.

### Publication Date

2017-10-01

### DOI

10.1007/s00249-017-1206-x

Peer reviewed



Published in final edited form as:

*Eur Biophys J.* 2017 October ; 46(7): 627–637. doi:10.1007/s00249-017-1206-x.

## Transmembrane helices containing a charged arginine are thermodynamically stable

Martin B. Ulmschneider<sup>1</sup>, Jakob P. Ulmschneider<sup>2</sup>, J. Alfredo Freites<sup>3</sup>, Gunnar von Heijne<sup>4</sup>, Douglas J. Tobias<sup>3</sup>, and Stephen H. White<sup>5,\*</sup>

<sup>1</sup>Institute for NanoBioTechnology & Department of Materials Science, Johns Hopkins University, Baltimore MD, 21218, USA

<sup>2</sup>Institute of Natural Sciences, Shanghai Jiao Tong University, Shanghai 200240, China

<sup>3</sup>Department of Chemistry and the Center for Biomembrane Systems, University of California, Irvine CA 92697-2025, USA

<sup>4</sup>Department of Biochemistry and Biophysics, Stockholm University, SE-106 91, Stockholm, Sweden

<sup>5</sup>Department of Physiology & Biophysics and the Center for Biomembrane Systems, University of California, Irvine CA 92697-4560, USA

### Abstract

Hydrophobic amino acids are abundant in transmembrane (TM) helices of membrane proteins. Charged residues are sparse, apparently due to the unfavorable energetic cost of partitioning charges into non-polar phases. Nevertheless, conserved arginine residues within TM helices regulate vital functions, such as ion channel voltage gating and integrin receptor inactivation. The energetic cost of arginine in various positions along hydrophobic helices has been controversial. Potential of mean force (PMF) calculations from atomistic molecular dynamics simulations predict very large energetic penalties, while in vitro experiments with Sec61 translocons indicate much smaller penalties, even for arginine in the center of hydrophobic TM helices. Resolution of this conflict has proved difficult, because the in vitro assay utilizes the complex Sec61 translocon, while the PMF calculations rely on the choice of simulation system and reaction coordinate. Here we present the results of computational and experimental studies that permit direct comparison with the Sec61 translocon results. We find that the Sec61 translocon mediates less efficient membrane insertion of Arg-containing TM helices compared to our computational and experimental bilayer-insertion results. In the simulations, a combination of arginine snorkeling, bilayer deformation, and peptide tilting is sufficient to lower the penalty of Arg insertion to an extent such that a hydrophobic TM helix with a central Arg residue readily inserts into a model membrane. Less favorable insertion by the translocon may be due to the decreased fluidity of the ER membrane compared to pure palmitoylcholine (POPC). Nevertheless, our results provide an explanation for the differences between PMF- and experiment-based penalties for Arg burial.

\*Correspondence to: Stephen H White, Department of Physiology and Biophysics, University of California at Irvine, Irvine, CA 92697-4560. stephen.white@uci.edu.

## Keywords

transmembrane helix; arginine; transfer free energy; lipid bilayer membrane; molecular dynamics; Sec61 translocon

---

## Introduction

Hydrophobicity scales that describe the interaction free energies of amino acids and polypeptides with fluid lipid bilayers are of primary importance for understanding the folding and stability of membrane proteins. Several physicochemical scales have been determined experimentally during the past twenty-five years, including partitioning of amino acid sidechain analogs from water into cyclohexane (1) and the partitioning of guest amino acids in host pentapeptides into *n*-octanol (2) and the lipid bilayer-water interface (3). Molecular dynamics simulations of the partitioning of amino acid sidechains into lipid bilayers also yield hydrophobicity scales derived from potentials of mean force (PMF) calculations (4). Such physical scales have enjoyed considerable success in the prediction of some aspects of membrane protein structures, such as the location of transmembrane (TM) helices (5) in amino acid sequences. However, these physical scales were necessarily derived without capturing the full complexity of proteins embedded in fluid lipid bilayer membranes.

Two important advances have provided biology-based hydrophobicity scales. Hessa et al. (6, 7) determined a hydrophobicity scale based upon an in vitro assay for Sec61 translocon selection of TM helices, while Moon and Fleming (8) determined a scale based upon the reversible refolding of the  $\beta$ -barrel membrane protein OmpLA into phospholipid vesicles. The translocon scale measures the partitioning of peptides between translocon and bilayer membrane whereas the OmpLA scale is related to water-to-bilayer partitioning. Nevertheless, these two scales offer a starting point for unifying biological, physical, and computation-based hydrophobicity scales. With unification in mind, we report here the results of simulation and experimental measurements of the partitioning into lipid bilayers of a series of hydrophobic helices containing a single arginine residue. Because the helices chosen were the same as ones used by Hessa et al. (6) in their determination of a biological hydrophobicity scale, we are able to compare directly physical, computational, and biological partitioning of a family of TM helices.

The biology-based measurements have not only enabled hydrophobicity scales to be derived for amino acid side chains attached to membrane proteins, they have also allowed the positional dependence of the scales within membranes to be determined. In the measurements of Hessa et al. (6), a guest amino acid was incorporated into a designed hydrophobic segment (H-segment), which was either inserted into or translocated across endoplasmic reticulum membranes by the Sec61 translocon in an in vitro translation assay. Quantification of the observed populations of inserted and translocated H-segments provided apparent free energies of insertion,  $G_{app}$ . Using this approach, a hydrophobicity scale was derived for amino acids placed in the middle of the H-segment (6). Furthermore, the dependence of  $G_{app}$  on the position of the guest residue within the H-segment was

determined (6, 7). In the measurements of Moon and Fleming (8), a guest residue was incorporated on the lipid-facing surface of OmpLA, and its contribution to the stability of the protein determined by experiments in which the equilibrium between the soluble unfolded form and the membrane-inserted folded form of the protein was monitored by fluorescence spectrometry. Systematic measurements of the twenty natural amino acids at a single sequence position yielded a hydrophobicity scale based on water-to-bilayer transfer free energies in the context of the OmpLA structure. In addition, the dependence of the transfer free energy on position within the membrane was determined for leucine and arginine (8).

How do these biological scales compare to physical and computational scales? Despite the diverse array of techniques used, the various scales are remarkably well correlated overall (9), but there are significant—and interesting—exceptions. The case of arginine insertion into membranes is an important example. Motivated by an early crystal structure of a voltage-gated ion channel that suggested that lipid-exposed arginine residues might make excursions deep into membranes during gating (10), a host of experiments and simulations were carried out to assess the penalty of burying positively charged arginine residues in membranes (4, 8, 11-24). The translocon-mediated insertion experiments of Hessa et al. (7, 11) and the water-to-membrane folding experiments of Moon and Fleming (8) suggest a remarkably small—a few kcal mol<sup>-1</sup>—energetic penalty for inserting an arginine residue into the middle of the sequence of a transmembrane segment. On the other hand, simulations have unanimously predicted a free energy penalty that is roughly an order of magnitude higher (4, 13, 14, 16, 18-20, 23).

What is the source of the discrepancy between the biology-based experiments and MD calculations for arginine-insertion energetics? One possibility is the assumption in MD calculations that the relevant process is partitioning between water and membrane so that the PMF can be calculated along a reaction coordinate that uses bulk water and the lipid bilayer hydrocarbon core as end states. But MD simulations of polyleucine segments containing a single arginine side chain (23) and of OmpLA (25), show that the Arg center-of-charge remains at or near the interface between the hydrocarbon core and the polar region of the lipid bilayer, irrespective of the position of the Arg C<sub>α</sub> in the polypeptide backbone. Another source of discrepancy is that the in vitro translocon-mediated insertion experiments of Hessa et al. (6, 7, 11) probe a complex process involving the partitioning of the H-segment between the interior of the translocon and the surrounding membrane (22, 23, 26, 27). Equilibrium water-to-bilayer partitioning thermodynamics more appropriate for direct comparison with simulations (24) are potentially available from the host-guest strategy of Moon and Fleming (8, 25), but structural information on the unfolded state that is necessary for guiding accurate modeling by MD simulations is presently lacking. Overall, the MD simulations and the translocon experiments are not equivalent. Translocon-aided insertion involves some kind of partitioning process between translocon and membrane, not simple partitioning between water and bilayer. Even if simulations include the translocon (22, 26, 27), one cannot know at present if they reflect accurately the reaction coordinate of the translocon-aided process. A logical step toward reconciling the translocon and simulation results is to use a model system that enables a side-by-side comparison of the water-to-bilayer and translocon-to-bilayer systems.

Here, we report a concerted experimental and MD simulation study of the membrane partitioning of arginine-containing peptides that prefer TM orientations, and for which the partitioning energetics can be obtained consistently from both experiment and simulation. By means of equilibrium MD simulations carried out on the microsecond time scale, we efficiently sample the states of arginine-containing hydrophobic peptides in a phospholipid bilayer environment, and obtain partitioning free energies without assuming a particular reaction coordinate (28, 29). Starting with a water-solvated unfolded configuration, the peptides readily fold at the lipid bilayer surface. Thereafter, water-soluble states are not observed, in agreement with the peptides' hydrophobic nature and the folding-partitioning of peptides such as melittin into membrane interfaces (30). We find that TM-inserted configurations are highly favored by the folded peptides. The relative populations of TM and surface-bound states are in excellent agreement with oriented circular dichroism measurements on multilamellar samples of similar composition. Irrespective of the peptide configuration and the location of the Arg in the peptide sequence, the arginine center-of-charge remains fully solvated by water molecules and lipid headgroups at the interface between the bilayer polar region and the hydrocarbon core as a result of Arg snorkeling, bilayer deformation, and peptide tilting. An unexpected finding is that TM helices containing arginine have a higher probability of insertion than observed in the Sec61 experiments, suggesting that the translocon partitioning process is different from direct partitioning.

## Results

Hessa et al. (6, 7) reported the insertion efficiencies of systematically designed 19-residue polypeptides, called H-segments, across the endoplasmic reticulum (ER) membrane by using the approach summarized in Fig. S1 (6, 7). In brief, H-segments were introduced into the large luminal P2 domain of the model protein leader peptidase (Lep) from *Escherichia coli*. Each H-segment was flanked by GGPG- and -GPGG tetrapeptides to 'insulate' it from the Lep carrier protein. Glycosylation sites were placed on either side of the segment to facilitate topology determination. The protein was then expressed *in vitro* in the presence of ER-derived dog pancreas rough microsomes. Because glycosylation only takes place in the interior of the microsome, membrane-inserted segments will be singly-glycosylated whereas translocated segments will be doubly-glycosylated. The insertion propensity  $p_{\text{TM}} = f_{1g}/(f_{1g} + f_{2g})$  of the segment can be determined by phospho-imager scans of SDS-PAGE gels that measure the fractions of singly ( $f_{1g}$ ) and doubly ( $f_{2g}$ ) glycosylated proteins. The results for H-segments containing a single Arg at various positions are summarized in Figure 1 (6), where we identify the H-segments by the position  $i$  of Arg ( $R_i$ ) in the segment. Arg carries a relatively small penalty for insertion at the center of the sequence (R10) that diminishes rapidly as the arginine side chain is moved towards the flanks of the H-segment.

### H-segment modifications for oriented circular dichroism and simulations

To simplify synthesis and to speed up the simulations, the insulating tetrapeptides GGPG- and -GPGG were replaced by a single Gly, because preliminary simulations revealed—as expected from the high cost of dehydrating peptide bonds that do not participate in intramolecular hydrogen bonds (2, 3)—very low transmembrane movements of the GGPG/

GPGG segments. Another modification of the model H-segments was the replacement of Ala at position 1 with Trp in order to simplify purification. This lowers the  $G_{app}$  of the segment by 0.3-0.4 kcal mol<sup>-1</sup>.

### Insertion of model H-segments via unrestrained molecular dynamics simulation

We carried out unrestrained atomistic molecular dynamics simulations of the Gly-flanked H-segment model peptides R4, R6, R8, and R10 to observe directly the folding, partitioning, and equilibrium dynamics of the peptides in the presence of a lipid bilayer. This approach allows direct determination of the insertion propensity and equilibrium configurational ensemble of the peptides, provided the relevant equilibrium states and transition barriers are thermally accessible. Because the arginine guanidinium can form multiple hydrogen bonds, these barriers are significant. We therefore elevated the temperature to 90 °C in the simulations. The validity of this high-temperature approach was verified experimentally (see SI Text).

Extended peptides were placed in the water phase ~15 Å from the surface of a POPC lipid bilayer and allowed to fold and partition freely into and out of the membrane. Figure 2 shows the folding-partitioning pathway of R8 and R10, but the other peptides behaved similarly. All peptides adsorbed rapidly and irreversibly to the surface of the bilayer, consistent with their experimentally observed insolubility (see SI Text). Once in the interface, all peptides folded into  $\alpha$ -helices, positioning themselves parallel to membrane at the carbonyl/hydrocarbon interface prior to insertion across the membrane. The formation of a surface bound helix (S state), which took between 100 and 800 ns, was a necessary prerequisite for TM insertion. Peptides R4, R6, and R8 remain stably inserted for the remainder of the simulation, with no exit events after TM insertion. R10 briefly returns once to the S state before re-inserting again into the TM state during the course of the 1.5  $\mu$ s simulation (see Figure 2). It is apparent from these simulations that the TM helix is the native configuration of the peptides in lipid bilayers.

Determination of transfer free energies requires both inserted and non-inserted states to be populated at equilibrium. To obtain accurate estimates of these equilibrium populations the peptide must insert and exit the membrane multiple times. We therefore elevated the temperature of the system further to make the non-inserted state thermally accessible (see SI text). We have previously demonstrated that partitioning kinetics increase exponentially with rising temperatures, without affecting the ratio of the inserted to surface bound populations, provided the peptides resist denaturation and remain fully folded (28, 29, 31-33). While the bilayer density decreases slightly with temperature the overall bilayer width remains unaffected, resulting in increased partitioning kinetics without affecting the value of the partitioning free energy.

Figure 3 shows the equilibrium simulation for R10 that has the arginine residue in the center of the sequence. The temperature of 140 °C was sufficient to overcome the transition barriers and made the interfacial state (S) accessible for R6 and R8. The results, summarized in Table 1, confirm the strong preference of all peptides for the TM configuration, which can therefore be taken as the native state at equilibrium, irrespective of the position of the Arginine in the H-segment. The data of Table 1 also show that the probability of insertion

decreases as Arg is moved toward the center of the model H segment, but not as strongly as previously observed in the translocon experiments (7).

### Bilayer response to arginine

How can the lipid bilayer accommodate an arginine residue in the middle of a TM helix? To address this question we analyzed the position of the arginine backbone (atoms C<sub>α</sub>, C, N, and O) and guanidinium sidechain (atoms N<sub>ε</sub>, C<sub>ζ</sub>, N<sub>η</sub>, and N<sub>θ</sub>), as a function of distance from the bilayer center, in conjunction with the density profiles of the chief structural groups of the bilayer (phosphates, glycerol-carbonyls, and hydrocarbon core). Figure 4, which shows the density profiles along the membrane normal for the key structural groups of the system, reveals that movement of Arg from the flanks of the peptide sequence to the center increases its burial depth. However, the charged guanidinium moiety is never fully buried in the hydrophobic core of the membrane and remains close to the glycerol-carbonyl/hydrocarbon interface. In contrast, the Arg backbone buries much more deeply, with an average displacement from the center of the bilayer of just  $\sim 5 \pm 2$  Å for R10, equivalent to one helical turn. These analyses show that Arg adapts to the membrane environment by the snorkeling of its guanidinium sidechain, while the entire helix shifts slightly towards the interface harboring the charged sidechain.

Analyses of the intermolecular interactions of the Arg residue with the surrounding lipids revealed that the guanidinium moiety is always closely hydrogen bonded to at least one phosphate (see Figure 5A). This has the effect of locally distorting the bilayer, by ‘pulling’ hydrogen-bonded phosphate lipid headgroups towards the glycerol carbonyls. This distortion is a clearly visible feature of the TM equilibrium configuration (see Figure 3), and is usually accompanied with a number of water molecules, or a small water ‘cone’ around the local distortion. Figure 4 shows a  $5 \pm 2$  Å shift along the membrane normal for the phosphate groups hydrogen bonded to the guanidinium sidechain. Close hydrogen bonding reduces the overall desolvation penalty of guanidinium. Together, the data suggest that ‘burial’ of the charged arginine sidechain is possible by a combination of local bilayer distortion, guanidinium snorkeling, and peptide shifting along the bilayer normal. No other effects or phenomena are needed to explain peptide insertion and guanidinium burial. These effects have also been observed in so-called GWALP23 peptides containing a single Arg near the TM helix center (34).

### Orientation of synthetic helices in lipid bilayers

The simulations indicated that all peptides insert as stable TM helices, regardless of the position of the Arg in the sequence. To verify these results experimentally, the ability of each peptide to insert across planar lipid bilayers was explored using oriented circular dichroism (OCD) spectroscopy. This method has been described in detail before (35). In brief, oriented multi-bilayer arrays were formed by depositing an organic solution containing both peptide and lipid onto quartz substrates. Highly oriented arrays form spontaneously after slow evaporation of the organic solvent followed by vapor-phase hydration at 100% relative humidity under nitrogen (36-38). Films formed in this way typically contain stacks of  $\sim 1000$  bilayers, which are highly aligned parallel to the quartz substrate, as determined by neutron diffraction (39).

The orientation of the synthetic peptides inside the planar POPC bilayer stacks was determined by recording CD spectra with the light beam perpendicular to the quartz substrate. Oriented CD spectra were obtained multiple times for each peptide. The results are shown in Figure 6, together with the theoretically predicted spectra for  $\alpha$ -helices aligned perpendicular and parallel to the bilayer normal. All peptides were found to be highly helical and aligned parallel to the membrane normal, with nearly identical spectra. Variation of the molar peptide-to-lipid ratio was found to have no effect on the results, with identical spectra for ratios in the range 1/100– 1/500 (Fig. S2). Unoriented spectra of the same peptides embedded in LUVs showed perfect helicity, indicating that the peptides are inserted as TM helices (Fig. S3). Thus synthetic peptide experiments and simulations agree on the equilibrium configurations of the peptides in a bilayer.

## Discussion

Arginine residues buried in TM segments are increasingly recognized as regulators of vital biological functions, such as voltage gating of ion channels (10) or integrin receptor signaling (40). But just how arginine can be accommodated in TM helices has remained controversial (23, 27, 41). This is primarily because the prohibitive free energy penalty for burial of arginine in the membrane interior, estimated from potential of mean force (PMF) calculations to be as high as 20 kcal mol<sup>-1</sup> at the membrane center (4, 13, 14, 16, 18-20, 23), has proved difficult to reconcile with the high efficiency with which arginine-containing peptides are inserted into biological membranes by the cellular translocon machinery (11). By challenging the Sec61 translocon with a set of systematically designed TM helices, Hessa et al. (6, 7) found that placing an arginine, or indeed two, at the center of a TM helix is not only possible, but carries a remarkably small ~2 kcal mol<sup>-1</sup> free energy penalty, compared to alanine (6, 7).

The apparent contradiction has proved difficult to resolve, because each method has caveats. The experimental assay probably measures the partitioning of TM segments between the translocon and the bilayer. Furthermore, little is known about the non-inserted state or if the GTP-powered ribosome, from which the nascent peptide chain is funneled into the translocon channel contributes to the insertion energetics. PMF calculations, on the other hand, are inherently reliant on the choice of an appropriate reaction coordinate, as well as the accuracy of molecular mechanics force fields, which determine all physicochemical properties of the system, and may not correctly reproduce the relevant solvent transfer energetics.

The ideal experiment would measure the folding and partitioning of a single peptide into and out of a lipid bilayer. The transfer free energy could then be determined directly from the relative equilibrium populations of the inserted and non-inserted configurations. The thermodynamic forces driving the associated folding-partitioning process have been carefully dissected by White and Wimley (42). However, it has proved impossible to date to construct such an experiment, chiefly because peptides that are sufficiently hydrophobic to partition into bilayers are generally insoluble (23).



Here, we used an approach that allows this single-peptide partitioning experiment to be performed in the computer using unbiased atomic-detail folding-partitioning simulations. Like a laboratory partitioning experiment, the simulated peptide is placed in water and allowed to fold, enter, and exit the bilayer freely. This allows direct observation of the equilibrium states of the system, defined by the peptide secondary structure, orientation, and location with respect to the bilayer at the inserted and non-inserted free energy minima. The relative populations of these states provide the insertion propensity and associated free energy. The only prerequisite for accurate thermodynamics is that the equilibria are sufficiently sampled and converged; this was checked carefully (see Fig. S4). The thermodynamic time-average of the key observables (i.e. the peptide helicity, orientation, and location in the bilayer) can in turn be measured experimentally via circular dichroism spectroscopy on identical peptides embedded in oriented lipid bilayers. Deconvolution of these averages then allows direct comparison of experimental and computational partitioning data.

This *in silico* partitioning method allowed us to compare the configurational equilibria and insertion propensity of hydrophobic peptides containing a single Arg residue (see Table 1). This comparison showed unambiguously that the peptides studied by Hessa et al., using the translocon assay, form stable TM helices in model membranes, regardless of the position of the arginine in the sequence (see Figure 6). The results indicate that, contrary to previous conclusions drawn from potential of mean force calculations (4, 13, 14, 16, 18-20, 23), the Sec61 translocon mediates less rather than more efficient membrane insertion of Arg-containing TM helices. This may be due to fundamental differences between spontaneous insertion from the membrane interface and translocon-guided partitioning (43, 44). However, it may also reflect on the different membrane composition of the ER, which contains >10% cholesterol as well as a significant protein content that may make it stiffer and thus less able to accommodate the defects required for arginine burial (see below).

How can the high penalties for arginine burial obtained from PMF calculations be reconciled with the relatively favorable insertion observed here? PMFs describe the variation of the free energy along a reaction coordinate. For arginine sidechains or their analogs this is generally chosen to be the burial depth along the membrane normal. The insertion free energy  $\Delta G$  is defined as the difference in free energy between the inserted and non-inserted states, respectively. A partitioning experiment will measure the free energy difference between these two states. For arginine embedded into a hydrophobic polypeptide segment, as described here, the inserted state is clearly a TM helix. The location and configuration of the non-inserted state is uncertain for the translocon or the OmpLA refolding experiments. For direct partitioning from water to bilayer we found the non-inserted state to be a helix bound to the interface of the bilayer, at the level of the lipid glycerol-carbonyl groups (c.f. Figure 4). The aqueous state is generally much higher in free energy, consistent with the experimentally observed insolubility of TM segments containing arginine (see SI text).

The free energy profiles for arginine side chain analogs have a consistent overall shape (Figure 7), with the penalty for arginine burial rising steeply with burial depth in the hydrophobic core of the bilayer. For R10, which has the arginine at the center of the TM segment, the average distance of the charged guanidinium side chain moiety from the bilayer

center is  $\approx 15 \pm 3 \text{ \AA}$  for the interface-bound (non-inserted) state and  $\approx 10 \pm 3 \text{ \AA}$  for the TM helix (inserted state). The calculated difference on the PMF free energy surface between these two states gives an unfavorable arginine side chain contribution to the overall insertion free energy of  $2\text{-}6 \text{ kcal mol}^{-1}$  (c.f. Figure 7) for all studies (4, 13, 14, 16, 18-20, 23). Both translocon experiments (7) and direct insertion studies (29) have shown that the favorable insertion free energy of hydrophobic peptides increases linearly with peptide length. Using these formulae to estimate the stabilization provided by the 18 residue ( $A_{12}L_6$ ) host peptide used here, gives  $G_{\text{insertion}} \approx -8 \text{ kcal/mol}$ , sufficient to overcome the penalty for adding an arginine sidechain (29). This means that while the PMF simulations might accurately capture the energetics of arginine burial, they cannot predict the actual positions of the relevant inserted and non-inserted minima on the free energy surface, which are required for calculating the experimentally relevant insertion free energy. These minima do not appear on the PMF profiles of sidechain analogs, because they are a feature of the hydrophobic TM helix to which the charged arginine sidechain is attached (see Figure 7). The peptide as well as the Arg must therefore be included in PMF calculations of this type.

A study by Allen and co-workers employed a setup where a single arginine residue was incorporated into a polyleucine helix that was chosen to be longer than the membrane width (13). The PMF for arginine translocation was constructed by pulling the helix, with its long axis parallel to the membrane normal, through the bilayer. The resulting transbilayer PMF was essentially identical to that of an arginine side chain analog on its own (13), which illustrates the importance of the choice of reaction coordinate. The unbiased simulations presented here show that the non-inserted free energy minimum for hydrophobic peptides containing an arginine residue is a surface-bound helix, with its long axis parallel to the membrane plane; the inserted state is a TM helix with a strong tilt angle  $\approx 37 \pm 12^\circ$  that facilitates arginine snorkeling as well as local deformation of the bilayer to allow deeper burial of the guanidinium group. In this context, a recent PMF approach by Sansom and coworkers looks promising (41). In that approach, the relevant orientations of peptides in the bilayer were first determined for each step along the membrane normal by extensive coarse-grain simulations and subsequently refined using atomistic simulations. The study confirmed the appropriateness of interface-bound and TM minima, for a related peptide.

Our equilibrium simulations show that arginine is never buried fully in the membrane core. Instead, the guanidinium moiety snorkels to the hydrated bilayer interface in a manner that involves bilayer distortion in its vicinity. Snorkeling of Arg to the headgroup region of the bilayer has been previously suggested as a means of lowering the insertion penalty of charged side chains (45, 46). Our results are broadly consistent with snorkeling, but in addition, we observed that a small number ( $2 \pm 1$ ) of lipid phosphates formed strong and persistent hydrogen bonds with the charged guanidinium group. This interaction ‘pulls’ a patch of the lipid head-group interface, including water molecules, towards the hydrophobic core, thus lowering the energetic penalty and increasing the burial depth of arginine further than would be possible by simple snorkeling alone. Finally, the whole peptide shifts by about one helical turn towards the interface accommodating the charged side chain. Together, these extreme-snorkeling effects sufficiently lower the penalty for arginine ‘burial’. Burial is thus not to be understood as ‘at the center of the bilayer’, but rather at the center of a TM helix (23). Because the capacity of the membrane to form defects is essential

for charge burial, insertion propensities are likely to be lower in less fluid membranes. This may explain why in the translocon assay, which measures insertion of polypeptide segments into the ER membrane, results in increased insertion penalties.

## Methods

### Peptide synthesis and purification

Peptides were solid-phase synthesized on a rink amide resin using Fmoc chemistry with increased coupling time. The core sequence was flanked by a glycine residue on either side and termini were acetylated and amidated respectively. The N-terminal alanine of each peptide was replaced by a tryptophan to allow concentration determination via UV absorption at 280 nm. Peptides were purified via reverse-phase high-pressure liquid chromatography (HPLC). Purity was checked via analytical HPLC and mass spectroscopy.

### Solution circular dichroism

Palmitoyloleoyl-phosphocholine (POPC) lipids were obtained from Avanti Polar Lipids (Alabaster, AL, USA). Samples were prepared by mixing stock solutions of peptide in trifluoroethanol and lipids in chloroform. The mixture was dried under a stream of nitrogen with subsequent overnight incubation under vacuum to remove all solvent traces. Vesicles were prepared by re-hydrating dry peptide/lipid films in 1 ml phosphate buffer at room temperature to reach a peptide concentration of 6  $\mu\text{M}$ . After 10 freeze-thawing cycles the vesicles were extruded 10 times through 0.1  $\mu\text{m}$  filters. The molar peptide/lipid ratio was 1/100. Peptide concentrations were quantified by the average absorbance of tryptophan at 280 nm using a molar extinction coefficient of  $\epsilon = 5600 \text{ M}^{-1}\text{cm}^{-1}$  (47). Circular dichroism measurements were carried out on a Jasco J-720 spectropolarimeter, using a 1 mm path length quartz cuvette. Six scans were averaged for each spectrum with bandwidth and resolution both set to 1 nm, and a response time of 2 s. Temperature was controlled with a Peltier device, and varied between 30 and 90  $^{\circ}\text{C}$ . Samples were equilibrated for 5 minutes at each temperature before collecting data following standard protocols (48).

### Oriented circular dichroism (OCD)

Measurements were carried on a Jasco J-720 spectropolarimeter, using a custom built OCD cell holder. Peptides and lipids were co-solubilized in trifluoroethanol (TFE) and applied drop-wise to quartz slides. After evaporation over night under vacuum the films were hydrated under nitrogen at 100% relative humidity for at least 48 hours before collecting spectra. Each film was measured by averaging 6 spectra from 8 rotation angles spaced 45 $^{\circ}$  apart at a temperature of 25  $^{\circ}\text{C}$ .

### Molecular dynamics simulations

All-atom simulations were performed using gromacs 4.5 ([www.gromacs.org](http://www.gromacs.org)) (49), and analyzed using hippo ([www.biowerkzeug.com](http://www.biowerkzeug.com)). All systems were simulated in the NPT ensemble using the OPLS all-atom (OPLS-AA) protein force field (50), in combination with the TIP3P water model (51), and OPLS-AA compatible united-atom lipid parameters (52). Atmospheric pressure of 1 bar was applied and the temperature range was 90 to 140  $^{\circ}\text{C}$  (see SI text for details).

## Supplementary Material

Refer to Web version on PubMed Central for supplementary material.

## Acknowledgments

This research was supported by a Marie Curie International Fellowship to M.B.U, grants from the National Institute of General Medical Science GM74737 (S.H.W.), Program Project GM86685 from NINDS and NIGMS (S.H.W.; D.J.T.), NSF grant CHE-0750175 (D.J.T.), and from the European Research Council (ERC-2008-AdG 232648), the Swedish Cancer Foundation, the Swedish Research Council, and the Swedish Foundation for Strategic Research (G.v.H).

## References

1. Radzicka A, Wolfenden R. Comparing the polarities of the amino acids: Side-chain distribution coefficients between the vapor phase, cyclohexane, 1-octanol, and neutral aqueous solution. *Biochemistry*. 1988; 27(5):1664–1670.
2. Wimley WC, Creamer TP, White SH. Solvation energies of amino acid sidechains and backbone in a family of host-guest pentapeptides. *Biochemistry*. 1996; 35:5109–5124. [PubMed: 8611495]
3. Wimley WC, White SH. Experimentally determined hydrophobicity scale for proteins at membrane interfaces. *Nature Struct Biol*. 1996; 3(10):842–848. [PubMed: 8836100]
4. MacCallum JL, Bennett WFD, Tieleman DP. Distribution of amino acids in a lipid bilayer from computer simulations. *Biophysical Journal*. 2008; 94:3393–3404. [PubMed: 18212019]
5. Jayasinghe S, Hristova K, White SH. Energetics, stability, and prediction of transmembrane helices. *J Mol Biol*. 2001; 312(5):927–934. [PubMed: 11580239]
6. Hessa T, et al. Recognition of transmembrane helices by the endoplasmic reticulum translocon. *Nature*. 2005; 433:377–381. [PubMed: 15674282]
7. Hessa T, et al. The molecular code for transmembrane-helix recognition by the Sec61 translocon. *Nature*. 2007; 450:1026–1030. [PubMed: 18075582]
8. Moon CP, Fleming KG. Side-chain hydrophobicity scale derived from transmembrane protein folding into lipid bilayers. *Proceedings of the National Academy of Sciences of the USA*. 2011; 108:10174–10177. [PubMed: 21606332]
9. MacCallum JL, Tieleman DP. Hydrophobicity scales: a thermodynamic looking glass into lipid-protein interactions. *Trends in Biochemical Sciences*. 2011; 36:653–662. [PubMed: 21930386]
10. Jiang YX, et al. X-ray structure of a voltage-dependent K<sup>+</sup> channel. *Nature*. 2003; 423:33–41. [PubMed: 12721618]
11. Hessa T, White SH, von Heijne G. Membrane insertion of a potassium channel voltage sensor. *Science*. 2005; 307:1427. [PubMed: 15681341]
12. Freites JA, Tobias DJ, von Heijne G, White SH. Interface connections of a transmembrane voltage sensor. *Proc Nat Acad Sci USA*. 2005; 102(42):15059–15064. [PubMed: 16217012]
13. Dorairaj S, Allen TW. On the thermodynamic stability of a charged arginine side chain in a transmembrane helix. *Proceedings of the National academy of Sciences*. 2007; 104(12):4943–4948.
14. MacCallum JL, Bennett WFD, Tieleman DP. Partitioning of amino acid side chains into lipid bilayers: Results from computer simulations and comparison to experiment. *J Gen Physiol*. 2007; 129(5):371–377. [PubMed: 17438118]
15. Doherty T, Su Y, Hong M. High-resolution orientation and depth of insertion of the voltage-sensing S4 helix of a potassium channel in lipid bilayers. *Journal of Molecular Biology*. 2010; 401:642–652. [PubMed: 20600109]
16. Vorobyov I, Li L, Allen TW. Assessing atomistic and coarse-grained force fields for protein-lipid interactions: the formidable challenge of an ionizable side chain in a membrane. *Journal of Physical Chemistry*. 2008; 112:9588–9602. [PubMed: 18636764]
17. Yoo J, Cui Q. Does arginine remain protonated in the lipid membrane? insights from microscopic pK<sub>a</sub> calculations. *Biophysical Journal: Biophysical Letters*. 2008; 94:L61–L63.

18. Johansson ACV, Lindahl E. Position-resolved free energy of solvation for amino acids in lipid membranes from molecular dynamics simulations. *Proteins*. 2008; 70:1332–1344. [PubMed: 17876818]
19. Johansson AC, Lindahl E. The role of lipid composition for insertion and stabilization of amino acids in membranes. *The Journal of Chemical Physics*. 2009; 130:185101–185101–185101–185108. [PubMed: 19449954]
20. Johansson ACV, Lindahl E. Titratable amino acid solvation in lipid membranes as a function of protonation state. *Journal of Physical Chemistry*. 2009; 113:245–253. [PubMed: 19118487]
21. MacCallum JL, Bennett WFD, Tieleman DP. Transfer of arginine into lipid bilayers is nonadditive. *Biophysical Journal*. 2011; 101:110–117. [PubMed: 21723820]
22. Gumbart J, Chipot C, Schulten K. Free-energy cost for translocon-assisted insertion of membrane proteins. *Proceedings of the National Academy of Sciences of the USA*. 2011; 108:3596–3601. [PubMed: 21317362]
23. Schow EV, et al. Arginine in membranes: the connection between molecular dynamics simulations and translocon-mediated insertion experiments. *Journal of Membrane Biology*. 2011; 239:35–48. [PubMed: 21127848]
24. Gumbart J, Roux B. Determination of membrane-insertion free energies by molecular dynamics simulations. *Biophysical Journal*. 2012; 102:795–801. [PubMed: 22385850]
25. Fleming PJ, Freitas JA, Moon CP, Tobias DJ, Fleming KG. Outer membrane phospholipase A in phospholipid bilayers: A model system for concerted computational and experimental investigations of amino acid side chain partitioning into lipid bilayers. *Biochim Biophys Acta*. 2011; 1818:126–134. [PubMed: 21816133]
26. Zhang B, Miller TF III. Hydrophobically stabilized open state for the lateral gate of the Sec translocon. *Proceedings of the National Academy of Sciences of the United States of America*. 2010; 107:5399–5404. [PubMed: 20203009]
27. Rychkova A, Vicatos S, Warshel A. On the energetics of translocon-assisted insertion of charged transmembrane helices into membranes. *Proceedings of the National Academy of Sciences of the USA*. 2010; 107:17598–17603. [PubMed: 20876127]
28. Ulmschneider MB, Smith JC, Ulmschneider JP. Peptide partitioning properties from direct insertion studies. *Biophysical Journal*. 2010; 98:L60–L62. [PubMed: 20550886]
29. Ulmschneider JP, Smith JC, White SH, Ulmschneider MB. In silico partitioning and transmembrane insertion of hydrophobic peptides under equilibrium conditions. *Journal of the American Chemical Society*. 2011; 133:15487–15495. [PubMed: 21861483]
30. Ladokhin AS, White SH. Folding of amphipathic  $\alpha$ -helices on membranes: energetics of helix formation by melittin. *J Mol Biol*. 1999; 285(4):1363–1369. [PubMed: 9917380]
31. Ulmschneider MB, et al. Spontaneous transmembrane helix insertion thermodynamically mimics translocon-guided insertion. *Nature communications*. 2014; 5:4863.
32. Ulmschneider MB, Doux JP, Killian JA, Smith JC, Ulmschneider JP. Mechanism and kinetics of peptide partitioning into membranes from all-atom simulations of thermostable peptides. *J Am Chem Soc*. 2010; 132(10):3452–3460. [PubMed: 20163187]
33. Ulmschneider JP, Doux JP, Killian JA, Smith JC, Ulmschneider MB. Peptide Partitioning and Folding into Lipid Bilayers. *J Chem Theory Comput*. 2009; 5(9):2202–2205. [PubMed: 26616605]
34. Vostrikov VV, Hall BA, Greathouse DV, Koeppe II RE, Sansom MSP. Changes in transmembrane helix alignment by arginine residues revealed by solid-state NMR experiments and coarse-grained MD simulations. *J Am Chem Soc*. 2010; 132:5803–5811. [PubMed: 20373735]
35. Wu Y, Huang HW, Olah GA. Method of oriented circular dichroism. *Biophys J*. 1990; 57(4):797–806. [PubMed: 2344464]
36. Hristova K, et al. An amphipathic  $\alpha$ -helix at a membrane interface: A structural study using a novel x-ray diffraction method. *J Mol Biol*. 1999; 290:99–117. [PubMed: 10388560]
37. Wimley WC, White SH. Designing transmembrane  $\alpha$ -helices that insert spontaneously. *Biochemistry*. 2000; 39(15):4432–4442. [PubMed: 10757993]
38. Hristova K, Dempsey CE, White SH. Structure, location, and lipid perturbations of melittin at the membrane interface. *Biophys J*. 2001; 80:801–811. [PubMed: 11159447]

39. Krepiy D, et al. Structure and hydration of membranes embedded with voltage-sensing domains. *Nature*. 2009; 462:473–479. [PubMed: 19940918]
40. Kim C, et al. Basic amino-acid side chains regulate transmembrane integrin signalling. *Nature*. 2012; 481:209–213.
41. Wee CL, Chetwynd A, Sansom MSP. Membrane insertion of a voltage sensor helix. *Biophysical Journal*. 2011; 100:410–419. [PubMed: 21244837]
42. White SH, Wimley WC. Membrane protein folding and stability: Physical principles. *Annu Rev Biophys Biomol Struct*. 1999; 28:319–365.
43. Cymer F, von Heijne G, White SH. Mechanisms of integral membrane protein insertion and folding. *J Mol Biol*. 2015:999–1022. [PubMed: 25277655]
44. Capponi S, Heyden M, Bondar AN, Tobias DJ, White SH. Anomalous behavior of water inside the SecY translocon. *Proc Natl Acad Sci U S A*. 2015; 112(29):9016–9021. [PubMed: 26139523]
45. Segrest JP, Deloof H, Dohlman JG, Brouillette CG, Anantharamaiah GM. Amphipathic Helix Motif - Classes and Properties. *Proteins*. 1990; 8:103–117. [PubMed: 2235991]
46. de Planque MRR, et al. Different membrane anchoring positions of tryptophan and lysine in synthetic transmembrane  $\alpha$ -helical peptides. *Biochemistry*. 1999; 274(30):20839–20846.
47. Pace CN, Vajdos F, Fee L, Grimsley G, Gray T. How to measure and predict the molar absorption coefficient of a protein. *Protein Sci*. 1995; 4(11):2411–2423. [PubMed: 8563639]
48. Greenfield NJ. Using circular dichroism collected as a function of temperature to determine the thermodynamics of protein unfolding and binding interactions. *Nature Protocols*. 2007; 1:2527–2535.
49. Berendsen HJC, van der Spoel D, van Drunen R. GROMACS: A new message-passing parallel molecular dynamics implementation. *Comp Phys Comm*. 1995; 91:43–56.
50. Jorgensen WL, Maxwell DS, Tirado-Rives J. Development and testing of the OPLS all-atom force field on conformational energetics and properties of organic liquids. *J Am Chem Soc*. 1996; 118:11225–11236.
51. Jorgensen WL, Chandrasekhar J, Madura JD, Impey RW, Klein ML. Comparison of simple potential functions for simulating liquid water. *J Chem Phys*. 1983; 79(2):926–935.
52. Ulmschneider JP, Ulmschneider MB. United atom lipid parameters for combination with the optimized potentials for liquid simulations all-atom force fields. *Journal of Chemical Theory and Computation*. 2009; 5:1803–1813. [PubMed: 26610004]

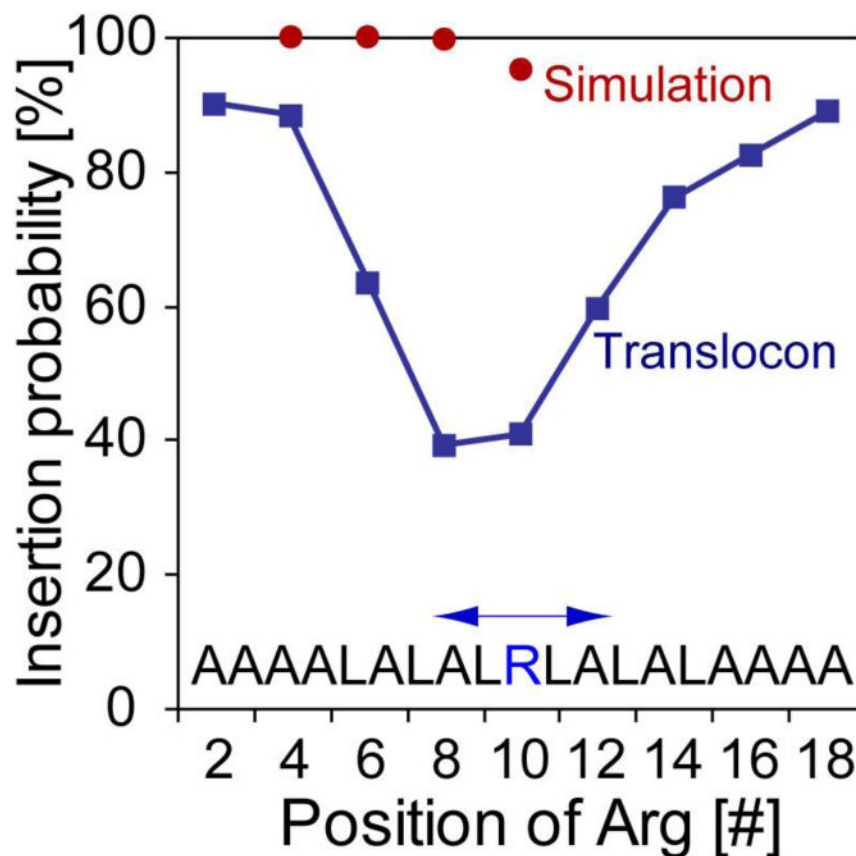


**Figure 1.**

Whole peptide partitioning propensity ( $P_{TM}$ ) as a function of arginine position along the sequence for  $R_i$  peptides ( $i = 4, 6, 8, \& 10$ ). The blue squares (■) correspond to  $P_{TM}$  values measured previously using a translocon assay, which also measured positions 2, 12, 14, 16, & 18 (6). Position 10 is at the center of the peptide. The computational partitioning data (●) ( $T = 140\text{ }^\circ\text{C}$ , see text) shows a maximum insertion penalty of  $-2.4\text{ kcal mol}^{-1}$  for an arginine in the center of the sequence (peptide R10, Table 1).

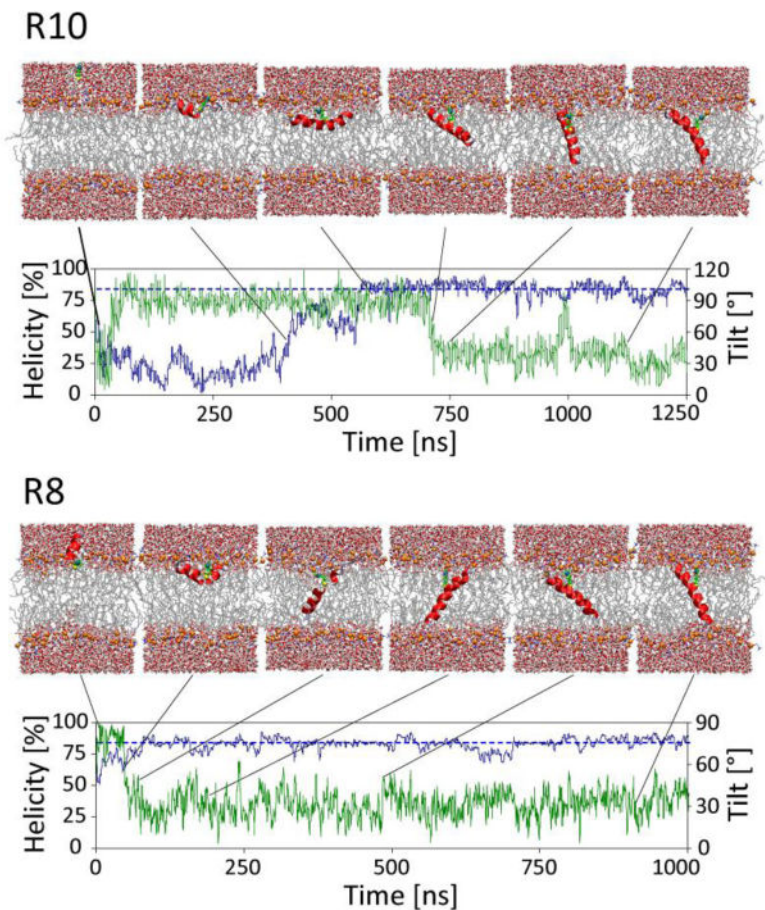


**Figure 2.**

Folding and partitioning simulations of the R10 and R8 peptides. The **upper panel** shows the folding-partitioning simulation of R10 in a POPC lipid bilayer at 90 °C. Equilibrium is reached after the peptide inserts into the bilayer at ~700 ns. After that the peptide remains chiefly inserted, with only one brief exit and re-entry event at ~1000 ns, apparent in the tilt angle (green). The peptide remains highly helical (blue). The **lower panel** shows the equivalent folding-partitioning simulation of R8 in a POPC lipid bilayer at 90 °C. This peptide inserts after folding rapidly at ~100 ns and remains fully inserted thereafter. To estimate the free energy of insertion from bilayer insertion/exit events the temperature needs to be elevated to make the interfacial state thermally accessible (see below). R6 and R4 behave similar to R8.



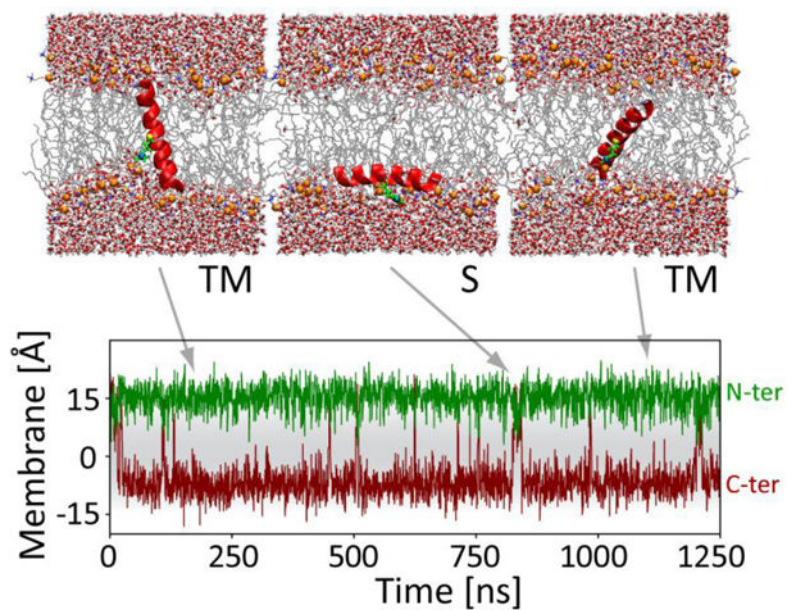


**Figure 3.** Equilibrium structures for R10 in a POPC bilayer at highly elevated temperatures ( $T = 140\text{ }^{\circ}\text{C}$ ). The Arg  $C_{\alpha}$  atom is indicated in yellow. In the TM configuration this atom is close to the center of the bilayer, while phosphates from the lipid headgroups are pulled down deep into the hydrocarbon core of the bilayer by the charged side-chain. Both weakly and strongly tilted peptides are observed in the TM configuration. After equilibrium is reached the peptide oscillates between surface bound (S) and transmembrane (TM) configurations. The TM configuration is the dominant state. Over 30 transitions are observed.

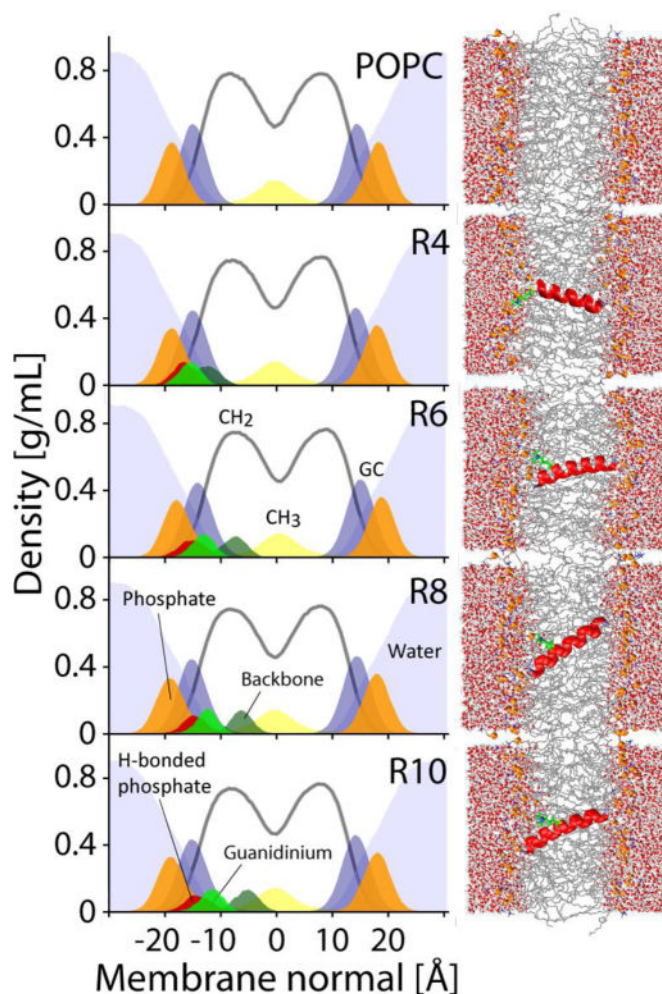


**Figure 4.**

Time averaged trans-bilayer density profile of Arg together with the key structural groups of the lipid bilayer (GC = glycerol carbonyls). The average is over the equilibrium part of the simulation. The figure shows the distributions of the charged guanidinium moiety and backbone of Arg together with the distribution of the phosphates hydrogen-bonded to Arg. Movement of Arg closer to the center of the sequence (Arg is in the center for R10) results in deeper burial of both the backbone and guanidinium groups. However, at no stage is the charged side-chain fully buried in the hydrophobic core of the bilayer. It is apparent from the figure that deeper burial is not possible, since the R10 peptide is able to accommodate Arginine at the center of the sequence. Further movement along the sequence results in similar results albeit for insertion of the peptide with the N-terminus.

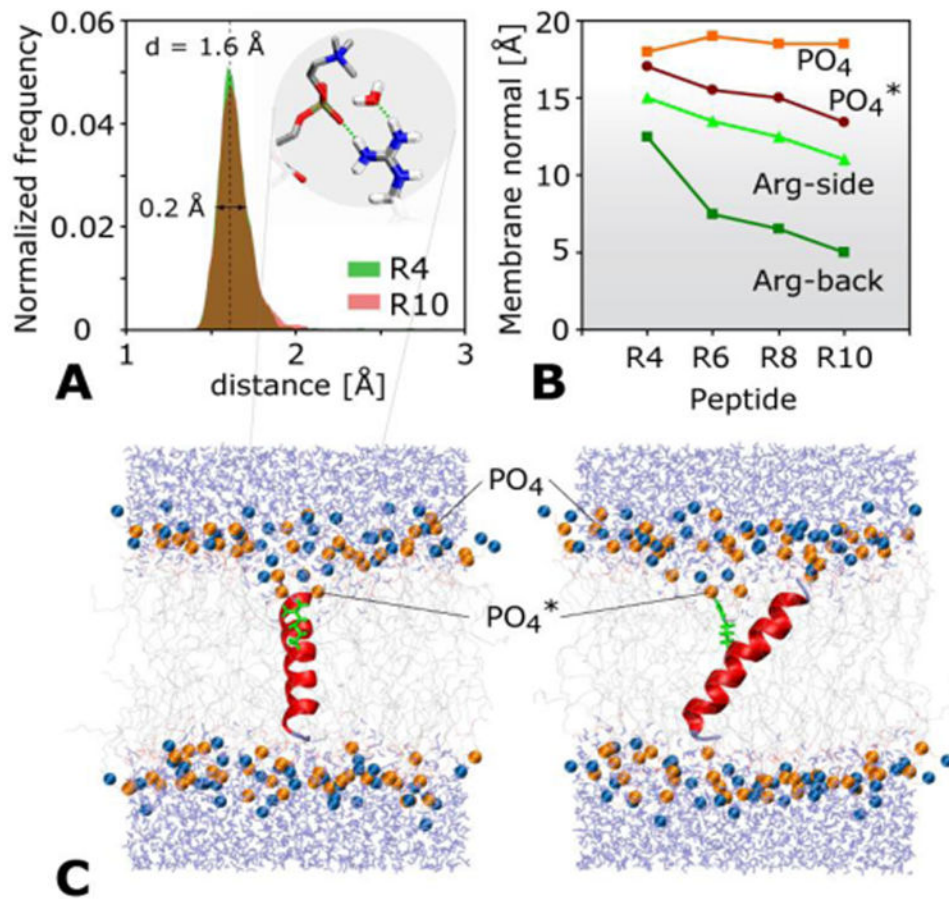


**Figure 5.**

Effect of arginine on the POPC bilayer. **A:** Minimum distance between the guanidinium side-chain of the R4 and R10 peptides and the phosphate groups of the lipid bilayer. The histogram is over the equilibrium part of the 90 °C simulations. The R6 and R8 peptides behave exactly similar. The peak of the distributions is at 1.6 Å. This indicates tight hydrogen bonding of the guanidinium group with at least one phosphate at all times, irrespective of the configuration in the bilayer and position of the arginine along the peptide sequence. The inset shows a close-up of a typical hydrogen bonding configuration from the simulations. In this example the guanidinium group forms hydrogen bonds with a lipid phosphate and water molecule. **B:** Variation of the mean distance from the membrane center for Arginine backbone (Arg-back), guanidinium side chain (Arg-side), and phosphate groups (PO<sub>4</sub>), and hydrogen-bonded phosphate groups (PO<sub>4</sub>\*) with respect to Arg position in the peptide sequence. Movement of Arg from the flanks of the sequence (R4) to the center (R10) results in deep burial of the Arg backbone in the hydrophobic core of the membrane. The burial is less pronounced for the charged guanidinium side chain (Arg side). Hydrogen-bonded phosphate groups are pulled down into the bilayer core with the guanidinium group. However, the overall distribution of phosphates (PO<sub>4</sub>) is not affected, demonstrating that the bilayer deformation is local, affecting only  $1.9 \pm 0.6$  phosphates. **C:** Visualization of the localized bilayer deformation. The difference in burial of the hydrogen-bonded phosphate

groups ( $\text{PO}_4^*$ ) is clearly visible. The right panel is the same frame rotated by  $90^\circ$  around the membrane normal, showing the strong tilt angle of the peptide.

Author Manuscript

Author Manuscript

Author Manuscript

Author Manuscript

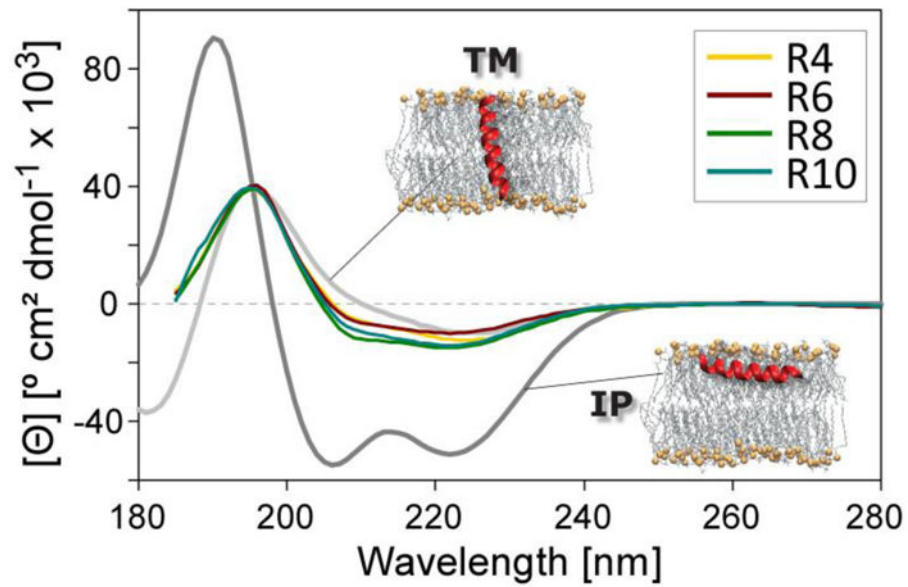


**Figure 6.** Oriented circular dichroism (OCD) spectra of the  $R_i$  ( $i = 4, 6, 8, \& 10$ ) peptides in stacked POPC lipid bilayers ( $[C]_{\text{peptide}} = 1 \text{ mg/mL}$ , peptide/lipid = 1/100, relative hydration = 100%). Theoretical reference spectra (at  $T = 25 \text{ }^\circ\text{C}$ ) for alpha-helical peptides oriented parallel (TM, tilt angle  $\approx 0^\circ$ ) and perpendicular (IP, tilt angle  $\approx 90^\circ$ ) to the membrane normal (coaxial to the light beam) are shown in grey. Decomposition of the spectra suggests TM populations of  $>95\%$  for all peptides. The peptide sequences are shown in Figure 1. All peptides are inserted as a membrane spanning alpha-helix.

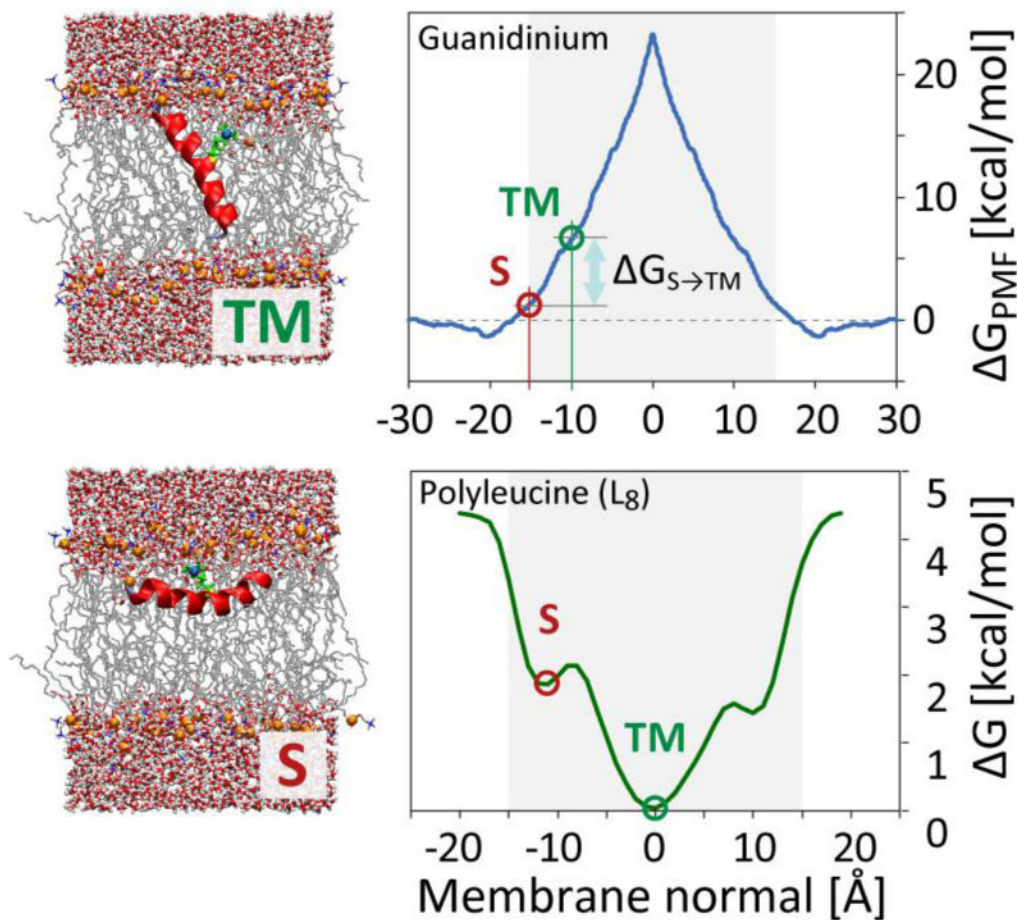


**Figure 7.**

Comparison of guanidinium PMF and hydrophobic-peptide free energy profiles. The transmembrane PMF of a guanidinium ion (from Schow et al. (23)) shows a steeply and monotonously rising free energy penalty with increasing burial depth from the lipid bilayer interface. The positions of the guanidinium groups for the interfacial (S) and transmembrane (TM) configurations are indicated on the surface, and are separated by  $\sim 5$  kcal/mol. The insertion free energy profile of a neutral polyleucine peptide ( $L_8$ ), shows that the interfacial and TM equilibrium positions are a general feature of hydrophobic peptides. For the peptides containing arginine, the water-to-bilayer partitioning equilibrium of the guanidinium group is constrained by these peptide equilibria.

**Table 1**

Comparison of the transmembrane insertion probability  $P_{TM}$  of 19 residue peptides containing arginine at various positions along the sequence. Insertion was determined via a translocon assay (SecY) into ER membranes, circular dichroism spectroscopy of synthetic peptides in oriented POPC lipid bilayers (OCD), and unrestrained all-atom peptide partitioning molecular dynamics simulations into POPC bilayers (MD).

Peptide	Sequence	$P_{TM}$ [%] <sup>‡</sup> (OCD)	$P_{TM}$ [%](Sec61) <sup>a</sup>	$P_{TM}$ [%](MD) <sup>‡</sup>
R4	AAARLALALALALALAAAA	>95	94.3	100.0 <sup>‡</sup>
R6	AAAALRLALALALALAAAA	>95	68.1	99.9
R8	AAAALALRLALALALAAAA	>95	35.3	99.8
R10	AAAALALALRLALALAAAA	>95	37.6	95.3

<sup>‡</sup>Computational determination for  $P_{TM}$  was only possible for the elevated temperature simulations ( $T = 140$  °C, see text).